High Precision Electromagnetic Momentum Positioning with Current Loop

Chao ZHANG*, Yufei ZHAO, and Hong WU

Labs of Avionics, School of Aerospace Engineering, Tsinghua University, Beijing, 100084, P. R. China

A novel high precision spatial positioning method utilizing the electromagnetic momentum, i.e., Electromagnetic Momentum Positioning (EMP), is proposed in this paper. By measuring the momentum of the electromagnetic field around the small current loop, the relative position between the sensor and the current loop is calculated. This method is particularly suitable for the application of close-range and high-precision positioning, e.g., data gloves and medical devices in personal healthcare, etc. The simulation results show that EMP method can give a high accuracy with the positioning error less than 1 mm, which is better than the traditional magnetic positioning devices with the error greater than 1 cm. This method lays the foundation for the application of data gloves to meet the accurate positioning requirement, such as the high precision interaction in Virtual Reality (VR), Augmented Reality (AR) and personal wearable devices network.

Keywords : Electromagnetic momentum positioning, current loop, wearable device, data glove, virtual reality

1. Introduction

Over the past few years, Virtual Reality (VR), Augmented Reality (AR) and other personal wearable devices have become popular [1]. Wearing head-mounted displays for VR, users need new input devices that can accurately track their hands and fingers in motion. Hence, accurately and efficiently tracking finger movements becomes highly important. Magnetic Field Positioning (MFP), which is proposed by Raab *et al.*, is one typical approach for continuous, accurate, and occlusion-free finger tracking [2]. Polhemus is one of the earliest systems utilizing MFP sensing, and can track objects with six degrees of freedom [1]. Some commercial products, such as Razer Hydra, use similar MFP approaches in combination with Inertial Measurement Units (IMUs) to enable game-controller-based tracking [3]. One major limitation of these works is that the strong 3-axis magnetic field has to be generated by their base stations. Moreover, the system design is overly complicated and suffers from the unavoidable zero-drifting and time asynchronization for wearable applications [4, 5].

To solve above issues, a novel positioning algorithm of small single-axis current loop by measuring electromagnetic momentum is proposed in this paper. The small current loop is considered as a simple, inexpensive, and very versatile antenna. The small loop with changing electric current will form the electromagnetic field distributed in the space according to Maxwell's equations [6, 7]. By detecting the change of electromagnetic momentum around the current loop, the relative spatial position between the sensor and the small loop can be determined. Moreover, with only small size single-axis current loop and 3-axis magnetic sensors, the EMP system can achieve high accuracy and real-time spatial localization. For the application of data gloves, the small current loops can be put on the fingertips, which forms a set of wearable 3D-input device.

2. Positioning Algorithm

The small current loop is equivalent to an infinitesimal magnetic dipole whose axis is perpendicular to the plane of the loop, i.e., the field radiated by an electrical small circular loop can be modeled as the same mathematical form as those radiated by an infinitesimal magnetic dipole [6, 7]. As shown in Fig. 1, the plane of the small loop is perpendicular to the z-axis and the loop center is defined as the origin of the coordinates, where ϕ is the azimuth angle and θ is the elevation angle.

The electromagnetic field around the small current loop can be expressed by the formulas derived in [7]. In the

*Corresponding author: Tel: +86-10-62797480
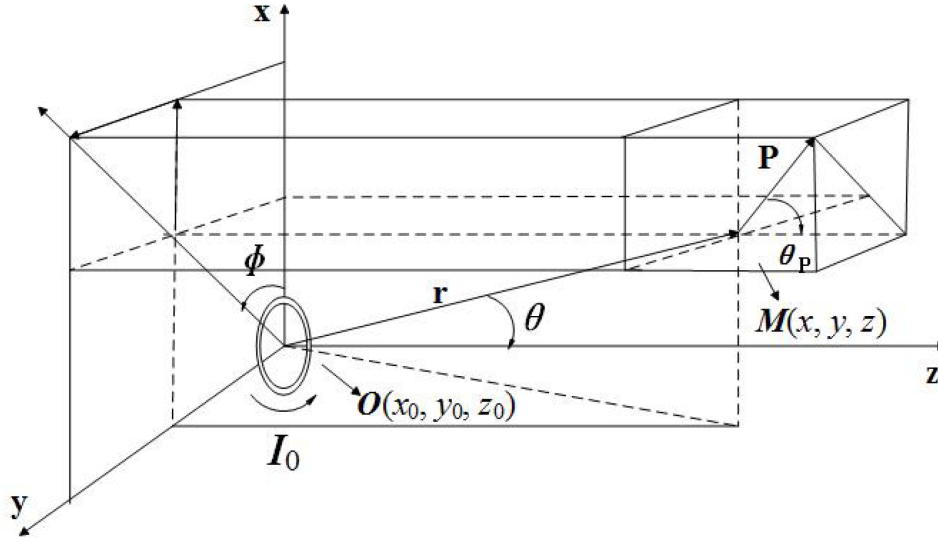Fax: +86-10-62785733, e-mail: zhangchao@tsinghua.edu.cn

Fig. 1. System structure with coordinates.

context of personal wearable devices or virtual reality applications, the expressions for the electromagnetic fields, as given in Chapter 5 of Ref. [7], can be simplified if the observations are made in the region very close to the small loop, i.e., $kr \ll 1$. Thus,

$$\begin{cases} H_r \simeq \dfrac{a^2 I_0 e^{-jkr}}{2r^3}\cos\theta \\[2ex] H_\theta \simeq \dfrac{a^2 I_0 e^{-jkr}}{4r^3}\sin\theta \\[2ex] H_\phi = E_r = E_\theta = 0 \\[2ex] E_\phi \simeq -j\dfrac{a^2 k I_0 e^{-jkr}}{4r^2}\sin\theta \end{cases} \qquad (1)$$

where, I_0 denotes the current amplitude, a is the radius of the small loop, k is the wave-number and r denotes the distance to the center of the small loop, $j = \sqrt{-1}$. The notation H and E with angle subscripts represent the components of magnetic and electric field strengths. If the receivers are near to the small loop and the frequency of the transmission signal is relatively low, the condition of $kr \ll 1$ can be satisfied [6, 7]. The values of the parameters can be referred to Table 1. According to the application scenarios of personal wearable devices, the

Table 1. Simulation Parameters.

Radius of the loop	4 mm
Current amplitude	0.05 A
Signal frequency	60 kHz
Magnetometer precision	1 nT

electromagnetic field around the small loop discussed in this paper actually can be classified as a quasi-stationary field [4].

It is well known that the momentum of the electromagnetic field at any point in space can be expressed as the cross-product of the electric and magnetic fields. For engineering applications, it is usually more convenient to write the momentum components in the Cartesian coordinate system. As the spatial geometry relation between the momentum density **P** and the small loop is depicted in Fig. 1, we get,

$$\mathbf{P} = (p_x, p_y, p_z) = \mathbf{E} \times \mathbf{H}^* \qquad (2)$$

where, "*" denotes the conjugate transform. Then, substituting Eqs. (1) into Eq. (2), the three components of momentum density **P** of the system can be obtained, which are simplified and expressed as the following.

$$\begin{cases} p_x = -\dfrac{3ka^4 I_0^2}{16r^5}j(\sin\theta(2\cos^2\theta - \sin^2\theta)\cos\phi) \\[2ex] p_y = -\dfrac{3ka^4 I_0^2}{16r^5}j(\sin\theta(2\cos^2\theta - \sin^2\theta)\sin\phi) \\[2ex] p_z = -\dfrac{3ka^4 I_0^2}{16r^5}j(\sin^2\theta\cos\theta) \end{cases} \qquad (3)$$

As for the measured data, at any point in the space, the 3-axis components of the magnetic field strength can be measured by a 3-axis magnetic sensor [8]. According to Maxwell's equations, the 3-axis components of the electric field can be obtained [9]. Moreover, the vector of the electric field is perpendicular to the magnetic field

vector. Hence, the measured value of the electric field **E** can also be obtained by the Hilbert transform of the magnetic field measured value **H** [8, 9].

2.1. Calculating ϕ and θ

According to Eqs. (3), the azimuth ϕ can be calculated by

$$\phi = \arctan \frac{p_y}{p_x}, \tag{4}$$

which means that the momentum vector **P** and the position vector **r** are in the same plane. As shown in Fig. 1, the elevation angle θ is not equal to θ_P, but we can calculate θ with the components in Eqs. (3). With Pythagorean theorem, we get,

$$\theta_P = \frac{\sqrt{p_x^2 + p_y^2}}{p_z} = \frac{2 - \tan^2 \theta}{3 \tan \theta} \tag{5}$$

Therefore,

$$\theta = \arctan \left(\frac{\pm \sqrt[4]{9 \frac{p_x^2 + p_y^2}{p_z^2} + 8} - 3 \frac{\sqrt{p_x^2 + p_y^2}}{L_z}}{2} \right) \tag{6}$$

Hence, the azimuth angle ϕ and the elevation angle θ are obtained.

2.2. Calculating the distance r

According to Eqs. (1), the modulus values of the total magnetic field strength **H** and electric field strength **E** can be calculated. Rewrite,

$$|\mathbf{H}|^2 + |\mathbf{E}|^2 = \frac{a^4 k^2 I_0^2}{16 r^4} + \frac{a^4 I_0^2}{16 r^6}(4\cos^2\theta + \sin^2\theta) \tag{7}$$

Fig. 2. (Color online) The experiment scenario.

With the measured values and the calculation above, $|\mathbf{H}|$, $|\mathbf{E}|$ and the elevation angle θ are obtained, then

$$r \approx \sqrt[3]{\frac{a^2 I_0 (4\cos^2\theta + \sin^2\theta)}{4(|\mathbf{H}|^2 + |\mathbf{E}|^2)^{1/2}}} \tag{8}$$

As shown in Fig. 1, in Cartesian coordinate system, the coordinates of any point $M(x, y, z)$ in the space can be calculated according to Eq. (6) and Eq. (8), which can be denoted as

$$\begin{cases} x = r \cdot \sin\theta \cos\phi \\ y = r \cdot \sin\theta \sin\phi \\ z = r \cdot \cos\phi \end{cases} \tag{9}$$

Hence, a novel method of spatial localization based on the momentum density has been established. Through measuring the electric and magnetic field of the small current loop, the spatial coordinates of the sensors to the loop source can be calculated.

3. Performance Evaluation

Figure 2 shows the experiment scenario for the near field application. The transmitter sources are composed of a set of variable single-axis coils which can generate the electromagnetic field in different frequencies. Even though the radiation resistance of a single-turn loop may be small, the overall value can be enhanced by increasing coil turns [7]. The receivers are the flux gate magnetic sensors for detecting the magnetic field strength generated by the small loops [10].

In order to evaluate the performance of the proposed positioning method, the positioning error of any point in space should be analyzed. In the simulation, a circular coil is chosen as the transmission source. The center of the coil is set in the origin point $O(0, 0, 0)$. All the simulation parameters are listed in Table 1. To confirm the validity of the simulation, an experiment is implemented which is shown in Fig. 2 and the measured data of the Signal to Noise Ratio (SNR) are listed in Table 2. The SNR of the magnetic sensor in 3-axis directions are denoted as η_x^{SNR}, η_y^{SNR} and η_z^{SNR}. In typical personal wearable devices, such as data gloves, the relative distance between the transmitter and receiver is
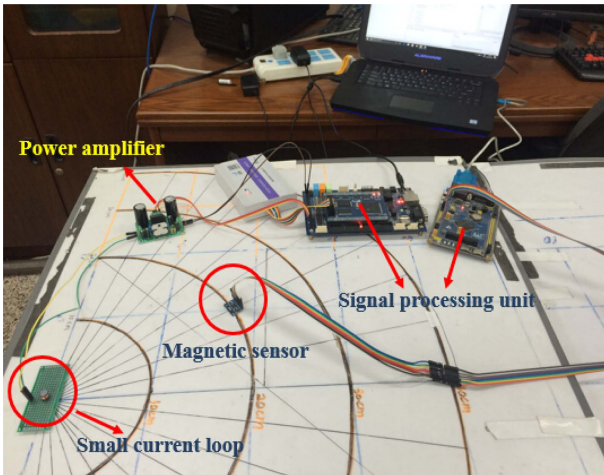
Table 2. Experimental Demonstration.

Distance (m)	0.2	0.3	0.4
η_x^{SNR} (dB)	30.39	24.53	21.01
η_y^{SNR} (dB)	28.65	25.02	19.64
η_z^{SNR} (dB)	29.86	25.17	19.19

usually within 0.4 m, i.e., the small loops can be put on the fingertips, and the receiver unit can be installed on the back of the hand or on the forearm [1]. Therefore, under this circumstance, the positioning accuracy of millimeter is required within the range of 0.4 m.

For our devices, according to the experimental data, the SNR can exceed 15 dB at the distance of 0.4 m from the source. In order to intuitively display the positioning performance of the EMP algorithm, we choose a certain elevation angle θ, e.g., $\theta = 45°$, and calculate the positioning Root Mean Square Error (RMSE) with the variation of SNR and distance. During this simulation, the normalized RMSE is defined as

$$\xi_{\text{RMSE}} = \frac{\sqrt{\frac{1}{N}\sum_{i=1}^{N}\left[(x_i - x_t)^2 + (y_i - y_t)^2 + (z_i - z_t)^2\right]}}{r} \quad (9)$$

where x_t, y_t, z_t are the true values of the position coordinates, x_i, y_i, z_i are the calculated values, N is the total number of measurements and r is the positioning distance which is between the small loop and the test point. The simulation results are shown in Fig. 3, where $N = 10^4$. From these results, it is clear that the positioning RMSE decreases significantly as the SNR increases. When the SNR is greater than 15 dB, the normalized RMSE is less than −26 dB. Hence, the algorithm can achieve the positioning accuracy of millimeter in the range of 0.4 m.
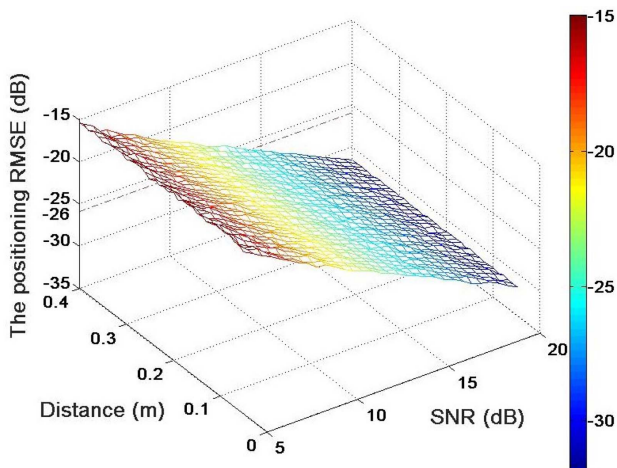

Fig. 3. (Color online) RMSE versus different range and SNR.

The electromagnetic of the small loop is an axial symmetric distribution, and the symmetric axis passes through center of the loop and is perpendicular to the loop plane [6, 7]. Figure 4 shows the position error versus different
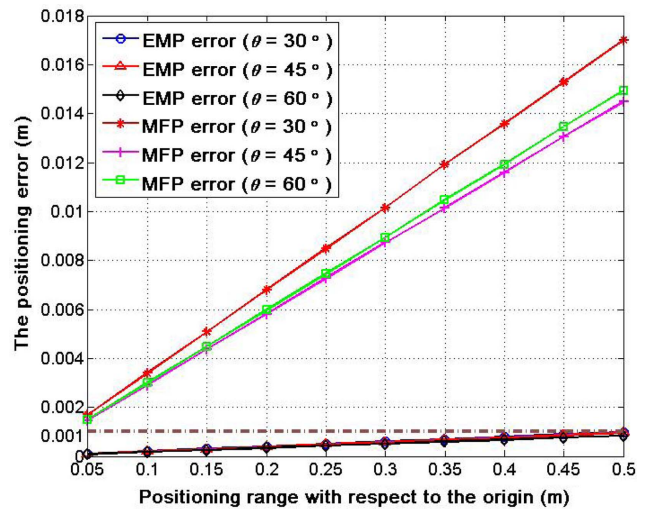

Fig. 4. (Color online) The position error versus range (m).
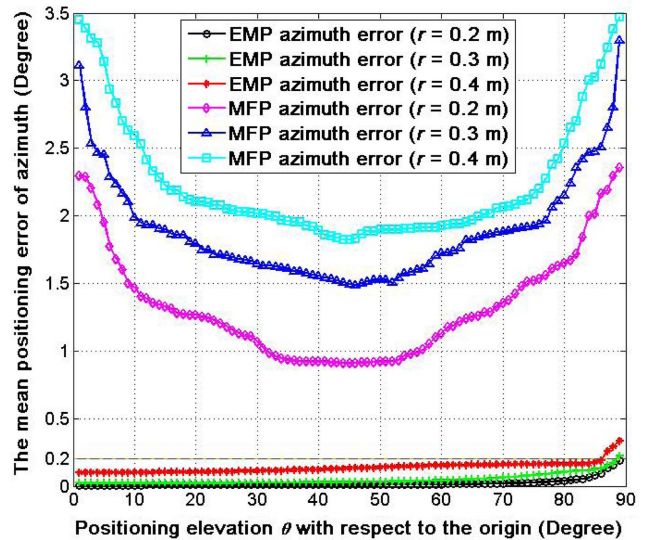

Fig. 5. (Color online) The azimuth error versus elevation (Degree).

ranges and Fig. 5 shows the azimuth error versus various elevation angles. These simulation results are compared with the traditional MFP algorithm, which is adopted widely in the applications, e.g., Polhemus [11]. The positioning error of EMP algorithm is smaller than the traditional MFP method, and it is more robust in the distance estimation. In terms of angle, the traditional MFP method has a larger error in the calculation of the azimuth angle in the same elevation angle, which will affect the calculation precision of the x, y, z coordinates. Under different elevation angle conditions, the azimuth calculation error of the EMP algorithm is less than 0.2 degree in the range of 0.4 m. Hence, EMP algorithm enables the capability of using single-axis coils to achieve high

precision of finger positioning.

4. Conclusion

In this paper, we present a novel electromagnetic momentum positioning method with small single-axis current loop. We leverage weak electromagnetic fields emitted from current loops for three dimensional positioning. Our evaluation reports an average positioning accuracy of millimeter within a sensing distance of 0.4 m. As head-mounted displays becoming accessible to the public, such as VR, the high precision finger-tracking system is becoming required for precise human machine interacting. The proposed EMP method with small current loop provides a promising solution.

Acknowledgement

References

[1] K.-Y. Chen, S. Patel, and S. Keller, CHI '16 Proceedings of the 2016 CHI Conference on Human Factors in Computing Systems, 1504 (2016).

[2] F. H. Raab, IEEE Trans. Geoscience and Remote Sensing **19**, 235 (1981).

[3] A. S. Mathur, IEEE Virtual Reality, 345 (2015).

[4] S.-S. Lee, J.-G. Choi, I.-H. Son, K.-H. Kim, D.-H. Nam, Y.-S. Hong, W.-B. Lee, D.-G. Hwang, and J.-R. Rhee, J. Magn. **16**, 449 (2011).

[5] D. J. Sturman and D. Zeltzer, IEEE Trans. Computer Graphics and Applications **14**, 30 (1994).

[6] S. Bae, Y.-K. Hong, J. Lee, J. Park, J. Jalli, G. S. Abo, H. M. Kwon, and C. K. K. Jayasooriya, J. Magn. **18**, 43 (2013).

[7] C. A. Balanis, Antenna Theory: Analysis and Design, Wiley, Hoboken, (1984) pp. 231-281.

[8] S. Yabukami, K. Arai, K. I. Arai, and S. Tsuji, J. Magn. **8**, 70 (2003).

[9] S. Ghnimi, A. Rajhi, and A. Gharsallah, J. Magn. **21**, 102 (2016).

[10] Y.-H. Kim, Y. Kim, C.-S. Yang, and K.-H. Shin, J. Magn. **18**, 159 (2013).

[11] F. H. Raab, E. B. Blood, T. O. Steiner, and H. R. Jones, IEEE Trans. Aerospace and Electron System **15**, 709 (1979).